

1 Estimation of sulfuric acid concentration using ambient ion 2 composition and concentration data obtained by Atmospheric 3 Pressure interface Time-of-Flight ion mass spectrometer

4 Lisa J. Beck¹, Siegfried Schobesberger², Mikko Sipilä¹, Veli-Matti Kerminen^{1,4} and Markku
5 Kulmala^{1,3,4,5}

6 ¹Institute for Atmospheric and Earth System Research/Physics, University of Helsinki, 00014 Helsinki, Finland

7 ²Department of Applied Physics, University of Eastern Finland, 70211 Kuopio, Finland

8 ³Aerosol and Haze Laboratory, Beijing Advanced Innovation Center for Soft Matter Sciences and Engineering,
9 Beijing University of Chemical Technology (BUCT), Beijing, China

10 ⁴Joint International Research Laboratory of Atmospheric and Earth System Sciences, School of Atmospheric
11 Sciences, Nanjing University, Nanjing, China

12 ⁵Faculty of Geography, Lomonosov Moscow State University, Moscow, Russia

13
14 *Correspondence to:* Lisa Beck (lisa.beck@helsinki.fi) and Markku Kulmala (markku.kulmala@helsinki.fi)

15 **Abstract**

16 Sulfuric acid (H₂SO₄, SA) is the key compound in atmospheric new particle formation. Therefore, it is crucial to
17 observe its concentration with sensitive instrumentation, such as chemical ionisation (CI) inlets coupled to
18 Atmospheric Pressure interface Time-of-Flight mass spectrometers (APi-TOF). However, there are environmental
19 conditions and physical reasons when chemical ionisation cannot be used, for example in certain remote places
20 or flight measurements with limitations regarding chemicals. Here, we propose a theoretical method to estimate
21 the SA concentration based on ambient ion composition and concentration measurements that are achieved by
22 APi-TOF alone. We derive a theoretical expression to estimate SA concentration and validate it with accurate CI-
23 APi-TOF observations. Our validation shows that the developed estimate works well during daytime in the boreal
24 forest (R² = 0.85), however it underestimates the SA concentration in e.g. Antarctic atmosphere during new
25 particle formation events where the dominating pathway for nucleation involves sulfuric acid and a base (R² =
26 0.48).

27 **1 Introduction**

28
29
30 Sulfuric acid (H₂SO₄, SA) is the key compound in atmospheric new particle formation (e.g. Weber et al., 1995,
31 1996; Birmili et al., 2003; Kulmala et al., 2004; Kuang et al., 2008; Kerminen et al., 2010; Wang et al., 2011;
32 Kulmala et al., 2014; Yao et al., 2018; Cai et al., 2021), therefore it is crucial to have accurate observations of its
33 concentration. However, ambient concentrations of H₂SO₄ are low, commonly less than a part per trillion by
34 volume (~2·10⁷ molecules cm⁻³), making it challenging to measure it. During the recent years there have been
35 instrumental developments towards a reliable detection of H₂SO₄ in the atmosphere, particularly via the
36 development of a Chemical Ionisation Atmospheric Pressure interface Time-of-Flight mass spectrometer (CI-
37

Deleted: concentrations

Deleted: spectrometry measurements (APi-TOF)

Deleted: CI-

Deleted: In these cases, it is important

Deleted: Here we

Deleted: The

Deleted: very

Deleted: with SA concentrations above 2·10⁶ cm⁻³.

Deleted: detect this concentration

Deleted: has

Deleted: clear steps

Deleted: the

50 API-TOF, Jokinen et al., 2012), using nitric acid as a reagent ion. Still, the measurement technique with CI-API-
51 TOF is relatively challenging, as a thorough calibration i.e. with sulfuric acid as proposed by Kürten et al. (2012),
52 is needed in order to get reliable numbers. Furthermore, the loss of sulfuric acid to surfaces, such as an inlet, and
53 the correct flow rates must be known and characterised.

54
55 During the past decade, Atmospheric Pressure interface Time-of-Flight mass spectrometers (APi-TOF, Junninen
56 et al., 2010) have been deployed in several measurement campaigns where the use of a CI inlet was either not
57 possible or desired. In these instances, the APi-TOF only observed the composition and concentration of ambient
58 ions. The APi-TOF is capable of directly sampling and detecting naturally charged gas-phase ions, including
59 molecular clusters, and is often being used to detect clustering processes as a first step of new particle formation
60 on a molecular basis (e.g. Schobesberger et al., 2013; Jokinen et al., 2018; Beck et al., 2021). While a CI-API-
61 TOF at best has a limit of detection around $\sim 10^4$ molecules cm^{-3} (\sim ppq level), the APi-TOF can detect
62 approximately 1% of the ambient ion concentration (Fig. 1, Junninen et al., 2010). With an average ion
63 concentration of ~ 1000 cm^{-3} per polarity (Hirsikko et al., 2011), the APi-TOF is measuring 10 ions $\text{cm}^{-3}\text{s}^{-1}$ with a
64 limit of detection of ~ 0.01 counts per second, hence 0.1 ions cm^{-3} . This corresponds to approximately pps level
65 ($100 \cdot 10^{-21}$), showing that the limit of detection of APi-TOF in comparison to CI-API-TOF is lower by five orders
66 of magnitudes.

67
68 A detailed description of the APi-TOF can be found in Junninen et al., (2010). Since concentrations of neutral
69 clusters are below the detection limit of CI-API-TOF in many atmospheric conditions and environments, using
70 the APi-TOF is currently the only way to directly detect atmospheric clustering. Therefore, if we can estimate
71 H_2SO_4 concentration particularly during initial steps of new particle formation, based on the same dataset, we can
72 readily get better insight into the process itself.

73
74 Since there are only limited long term observations of H_2SO_4 concentrations, several proxies on this concentration
75 have also been developed (e.g. Petäjä et al., 2009; Mikkonen et al., 2011; Lu et al., 2019; Dada et al., 2020). These
76 proxies attempt to approximate the ambient H_2SO_4 concentrations using more readily measured quantities, in
77 particular the sulfur dioxide concentration, (UV) radiation intensity and pre-existing particle number size
78 distribution that can be used to calculate the condensation sink for gas-phase H_2SO_4 . In circumstances where the
79 required data for H_2SO_4 proxies are not available, but measurements with an APi-TOF were conducted, the H_2SO_4
80 concentration can be obtained from the ion mass spectra. A first attempt of estimating the sulfuric acid
81 concentration via the concentration of atmospheric ions was introduced by Arnold and Fabian (1980), followed
82 by Eisele (1989) under the assumption that most H_2SO_4 molecules are charged by reacting with NO_3^- .

83
84 Motivated by the reasonings outlined above, we derive here an expression to estimate H_2SO_4 concentration based
85 primarily on APi-TOF observations and validate it.

Deleted: or so

Deleted: this instrument

Deleted: case we are able to estimate the H_2SO_4 concentration from its influence on the ion mass spectra obtained by APi-TOF, that estimate may be more accurate than the use of H_2SO_4 proxies.

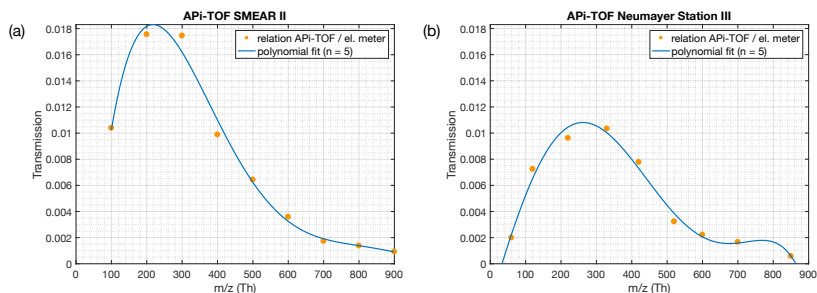


Figure 1 Ion transmission of the API-TOFs used in this study. The transmission efficiency was determined via production of charged particles with a NiCr wire. The concentration of the size selected ions with a Hermann nano differential mobility analyser (HDMA, Hermann, 2000) were measured with an electrometer and an API-TOF in parallel. A more detailed description can be found in Junninen et al. (2010). Panel (a) shows the transmission efficiency of the API-TOF used for measurements at the SMEAR II Station, Hyytiälä, Finland. Panel (b) shows the transmission efficiency used for measurements at the Neumayer Station III.

2 Theoretical estimation of sulfuric acid concentration with bisulphate ion and H₂SO₄ clusters

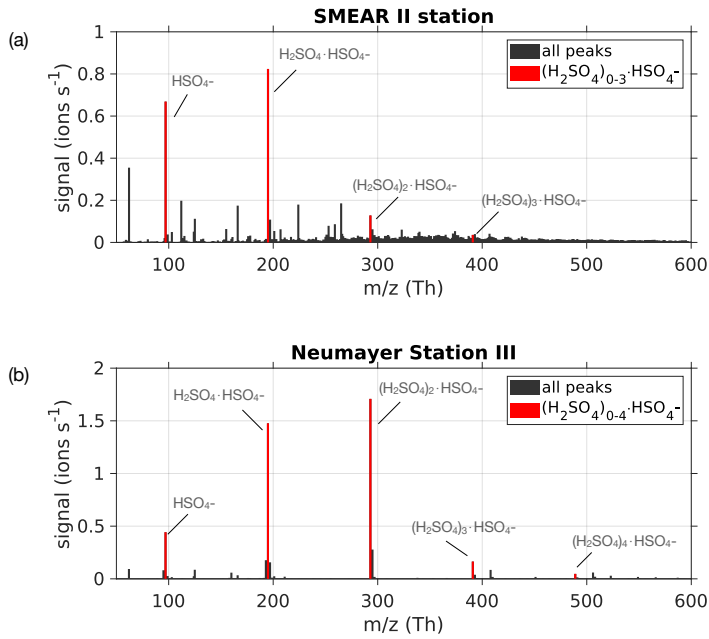
Ambient ion mass spectra ~~have usually~~ clear evidence of gas-phase H₂SO₄, predominantly in the form of bisulphate ion (HSO₄⁻) and its adducts involving H₂SO₄, forming so-called dimers (H₂SO₄·HSO₄⁻) as well as larger clusters (Ehn et al., 2010). These are due to the efficient scavenging of negative charge by ambient H₂SO₄ via proton donation, and due to the high stability of the sulfuric acid-bisulphate ion clusters, in particular for the dimer (Ortega et al., 2014). In order to estimate the sulfuric acid concentration (H₂SO₄) using the measured naturally charged ions (see Fig. 2), we ~~approximate this~~ concentration by following the bisulphate ion HSO₄⁻, herein denoted SA_{monomer}, the dimer cluster H₂SO₄·HSO₄⁻ (SA_{dimer}) and trimer cluster (H₂SO₄)₂·HSO₄⁻ (SA_{trimer}). Any other H₂SO₄-containing ion clusters, in particular those larger than the SA_{trimer}, typically occur at much smaller concentrations and will be neglected ~~here~~.

Deleted: commonly

Deleted: contain

Deleted: 1

Deleted: theoretically explain that



119
 120 **Figure 2** (a) Mass spectrum from 50 to 600 Th measured with the API-TOF on 24 May 2017 during the time period 08:00 –
 121 18:00 (local time) at SMEAR II station, Hyytiälä, Finland. (b) Mass spectrum from 14 January 2019 between 08:00 and 18:00
 122 (local time) at Neumayer Station III, Antarctica during a new particle formation event. The bisulphate ion HSO_4^- and H_2SO_4
 123 clusters containing it were used for the estimation of H_2SO_4 concentration, and are coloured in red.

124
 125
 126 If we assume that the concentration of $\text{SA}_{\text{monomer}}$ depends generally on its production rate (P_1) and that its loss is
 127 by condensation onto aerosol particles (condensation sink, CS_a), to the SA_{dimer} , when clustering with another H_2SO_4
 128 molecule, and to ion-ion recombination with positive ions (N_{pos}), we get the following equation for the $\text{SA}_{\text{monomer}}$
 129 concentration:

$$\frac{d[\text{SA}_{\text{monomer}}]}{dt} = P_1 - \text{CS}_a \cdot [\text{SA}_{\text{monomer}}] - P_2 - \alpha \cdot [\text{SA}_{\text{monomer}}] \cdot N_{\text{pos}}, \quad (1)$$

130
 131
 132 where $P_2 = k_1 \times [\text{SA}_{\text{monomer}}] \times [\text{H}_2\text{SO}_4]$ is the dimer production rate due to $\text{SA}_{\text{monomer}}\text{-H}_2\text{SO}_4$ collisions, α (≈ 1.6
 133 $\times 10^{-6} \text{ cm}^3 \text{ s}^{-1}$) is the ion-ion recombination coefficient (Kontkanen et al., 2013), and the collision rate k_1 is assumed
 134 to be constant.

Deleted: 1

Deleted:)

Deleted: the

Deleted:) and its loss

Deleted: ,

Deleted: this

142 For the dimer concentration we consider the production P_2 , the loss due to CS, the clustering of the SA_{dimer} with
 143 H_2SO_4 with a rate constant k_2 , and the ion-ion recombination:

$$144 \frac{d[SA_{dimer}]}{dt} = P_2 - CS \cdot [SA_{dimer}] - k_2 \cdot [SA_{dimer}] \cdot [H_2SO_4] - \alpha \cdot [SA_{dimer}] \cdot N_{pos} \quad (2)$$

145
 146 And with substituting P_2 , eq. 2 for SA_{dimer} changes to:

$$147 \frac{d[SA_{dimer}]}{dt} = k_1 \cdot [SA_{monomer}] \cdot [H_2SO_4] - CS \cdot [SA_{dimer}] - k_2 \cdot [SA_{dimer}] \cdot [H_2SO_4] - \alpha \cdot [SA_{dimer}] \cdot N_{pos} \quad (3)$$

148
 149 Finally, to produce SA_{trimer} we consider the collision of the SA_{dimer} with H_2SO_4 and the loss to the CS, and ion-ion
 150 recombination. For the sake of completeness, we would additionally have to consider the loss of $SA_{trimers}$ to form
 151 the tetramer $(H_2SO_4)_3 \cdot HSO_4$, however this additional term is rather small and will therefore be neglected in this
 152 derivation. Therefore, we get the simplified equation for SA_{trimer} :

$$153 \frac{d[SA_{trimer}]}{dt} = k_2 \cdot [SA_{dimer}] \cdot [H_2SO_4] - CS \cdot [SA_{trimer}] - \alpha \cdot [SA_{trimer}] \cdot N_{pos} \quad (4)$$

154
 155 For simplification, we consider a pseudo-steady state condition for both dimers and trimers by setting the left-
 156 hand side of eqs. (3) and (4) to be zero, which is justified when the dimer and trimer concentrations change at
 157 rates smaller than their overall production and loss rates. Thereby, from eq. (3) we obtain:

$$158 \begin{aligned} & k_1 \cdot [SA_{monomer}] \cdot [H_2SO_4] \\ & = CS \cdot [SA_{dimer}] + k_2 \cdot [SA_{dimer}] \cdot [H_2SO_4] + \alpha \cdot [SA_{dimer}] \cdot N_{pos} \end{aligned} \quad (5)$$

159
 160 and from eq. (4) we obtain:

$$161 k_2 \cdot [SA_{dimer}] \cdot [H_2SO_4] = CS \cdot [SA_{trimer}] + \alpha \cdot [SA_{trimer}] \cdot N_{pos} \quad (6)$$

162
 163 If we now deploy equation (6) in equation (5) and solve for H_2SO_4 , the result is:

$$164 k_1 \cdot [SA_{monomer}] \cdot [H_2SO_4] = CS \cdot [SA_{dimer}] + CS \cdot [SA_{trimer}] + \alpha \cdot [SA_{dimer}] \cdot N_{pos} + \alpha \cdot [SA_{trimer}] \cdot N_{pos} \quad (7)$$

$$165 [H_2SO_4] = \frac{(CS + \alpha \cdot N_{pos}) \cdot ([SA_{dimer}] + [SA_{trimer}])}{k_1 \cdot [SA_{monomer}]} \quad (8)$$

Deleted: and

Deleted:],

Deleted:],

Deleted: .

Deleted: -,

Deleted:],

Deleted:],

Deleted:],

Deleted: $\frac{CS \cdot ([SA_{dimer}] + [SA_{trimer}])}{k_1 \cdot [SA_{monomer}]}$

175 Besides the steady-state assumption, it should be noted that in deriving eq. 8 monomers, dimers and trimers were
176 assumed to have the same loss rate (CS) onto pre-existing aerosol particles. This causes an additional, yet minor,
177 uncertainty in estimated H₂SO₄ concentrations, as such loss rates are dependent on the size/mass of the clusters
178 (e.g. Lehtinen et al., 2007; Tuovinen et al., 2021). According to Tuovinen et al. (2021), the CS of H₂SO₄ clusters
179 decreases with increasing number of H₂SO₄ molecules. The study shows that the CS of the SA_{dimer} clustered with
180 ammonia decreases to 68% (compared to one H₂SO₄ molecule) and for SA_{pentamer} with four ammonia molecules
181 to 42%. However, the order of magnitude of the CS remains the same, and the effect on the estimation of the
182 H₂SO₄ concentration is assumed to be negligible. Additionally, the CS for ions is higher than for neutral
183 compounds. The enhancement of CS has shown to reach a maximum value of 2 when the pre-existing particles
184 are < 10 nm and decreases to 1 when the pre-existing particles are > 100 nm, as shown by Mahfouz and Donahue
185 (2021).

186
187 Furthermore, the derivation neglects the losses of SA_{trimer} to the SA_{tetramer} and larger clusters, as well as the
188 clustering of sulfuric acid ion clusters with water and base molecules, such as NH₃. Those simplifications can
189 cause an underestimation of the H₂SO₄ concentration with the presented method. If necessary, the method can
190 easily be adapted, and bigger clusters can be included in the equation. ▼

Deleted:).

191
192 From equation 8 we also see that the concentration of H₂SO₄ is proportional to relative concentrations of sulfuric
193 acid monomers, dimers and trimers clustered with the bisulphate ion:

$$[H_2SO_4] \sim \frac{[SA_{dimer}] + [SA_{trimer}]}{[SA_{monomer}]} \quad (9)$$

195
196 To estimate the H₂SO₄ concentration with the ion mode APi-TOF, we can therefore use this theoretical approach,
197 in particular Eq. 8. For the collision rate of H₂SO₄ with HSO₄⁻ we use $k_1 = 2 \cdot 10^{-9} \text{ cm}^3 \text{ molecule}^{-1} \text{ s}^{-1}$ as in Lovejoy
198 et al., (2004). The value of CS is calculated based on Kulmala et al., (2012). Even if the CS was unknown due,
199 for example, to the lack of particle measurements, the daytime variability of the H₂SO₄ concentration could still
200 be estimated only by using the relation of the H₂SO₄-containing cluster with HSO₄⁻, as it is proportional to the
201 H₂SO₄ concentration (see eq. 9). If the concentration of positive small ions is not available, it can be assumed to
202 be in the range of 500 – 1000 cm⁻³ which is a reasonable approximation for the average concentration (Hirsikko
203 et al., 2011).

204
205 As the transmission of clusters within an APi-TOF depends on the tuning of the instrument and on the pressures
206 within its chambers, the transmission efficiency needs to be considered, in order to get reliable concentrations of
207 the SA_{monomer}, SA_{dimer}, and SA_{trimer}. Fig. 1 shows the transmission efficiency curve of the APi-TOF used at the
208 SMEAR II station and Neumayer Station III. The effect of applying the transmission correction to the different
209 SA clusters is depicted in Fig. 3 for the time series at the SMEAR II station. All ion signals were normalised to a
210 transmission of 1%. As can be determined from Fig. 1a, the SA_{monomer}'s transmission at SMEAR II was ~1%,
211 while the dimer and trimer were corrected by a factor of 1/1.8 and 1/1.65, respectively. The correction was also
212 applied on the ions measured at the Neumayer Station III according to the APi-TOF's transmission (Fig. 1b).

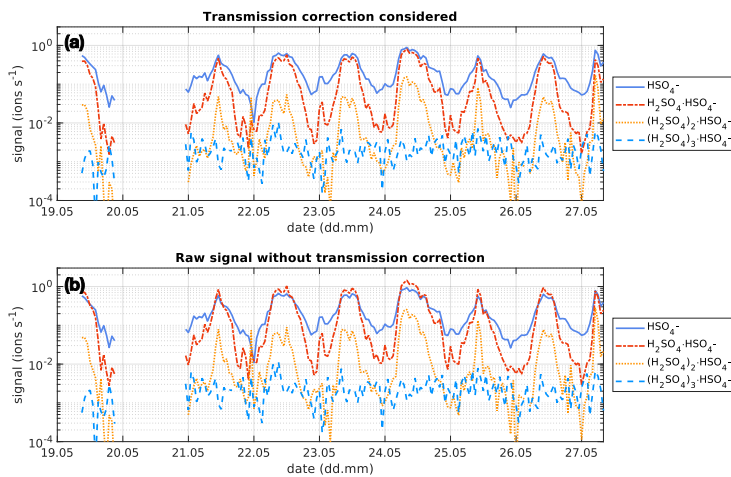


Figure 3 Time series of the bisulphate ion (HSO_4^- , $\text{SA}_{\text{monomer}}$), H_2SO_4 clustered with bisulphate ($\text{H}_2\text{SO}_4\cdot\text{HSO}_4^-$, SA_{dimer}), two H_2SO_4 molecules clustered with the bisulphate ion ($(\text{H}_2\text{SO}_4)_2\cdot\text{HSO}_4^-$, $\text{SA}_{\text{trimer}}$) and three H_2SO_4 molecules clustered with the bisulphate ion ($(\text{H}_2\text{SO}_4)_3\cdot\text{HSO}_4^-$, $\text{SA}_{\text{tetramer}}$) between 19 and 27 May 2017 at SMEAR II station, Hyytiälä, Finland. The concentration is given in ions s^{-1} as measured by the API-TOF. The upper panel shows the concentration of the clusters considering the transmission efficiency of the instrument (see Fig. 1). The lower panel shows the concentration of the clusters without that correction and assuming a constant transmission efficiency of 1% for all ions.

3 Validation

We tested the expression derived above using a dataset collected during inter-comparison measurements at the SMEAR II station in Hyytiälä, Finland (Hari and Kulmala, 2005). In Fig. 4 we show the time series of the observed H_2SO_4 concentrations, measured with a CI-API-TOF. The CI-API-TOF was calibrated for sulfuric acid, based on the method by Kürten et al., (2012) and resulted in a calibration factor of 2.5×10^9 . Additionally, we show the estimated sulfuric acid concentration based on API-TOF measurements together with Eq. 8 and the sulfuric acid proxy concentration (Dada et al., 2020). The concentration of positive ions for the estimated sulfuric acid concentration was obtained from a Neutral cluster and Air Ion Spectrometer (NAIS, Airel Ltd., Mirme and Mirme, 2013).

The estimated H_2SO_4 concentration agrees with the measured one during most of the daytime. Between 06:00 and 18:00 local time, the correlation (R^2) between the estimated and measured H_2SO_4 concentration is equal to 0.85 with a root mean square error (RMSE) of $4.12 \times 10^5 \text{ cm}^{-3}$. During night-time, the corresponding values are 0.85 and $3.23 \times 10^5 \text{ cm}^{-3}$ (Table 1).

The scatter plot in Fig. 5 shows that the estimated H_2SO_4 concentrations agree well with the observed one when H_2SO_4 concentrations are larger than $2 \times 10^6 \text{ cm}^{-3}$, demonstrating that our method works particularly well at the SMEAR II station during conditions that favour the formation of H_2SO_4 -containing clusters.

Deleted: 2

Deleted: estimated and

Deleted: CI-API-TOF measurements, respectively. The estimated H_2SO_4 concentration agrees well with the measured one during most of the daytime. During night-time, however, the estimated H_2SO_4

Deleted: seems to be considerably higher than the measured one. This could be because the SA_{dimer}

Deleted: is considerably lower than the $\text{SA}_{\text{monomer}}$ (see Fig. 3)

Deleted: 4

Deleted: the

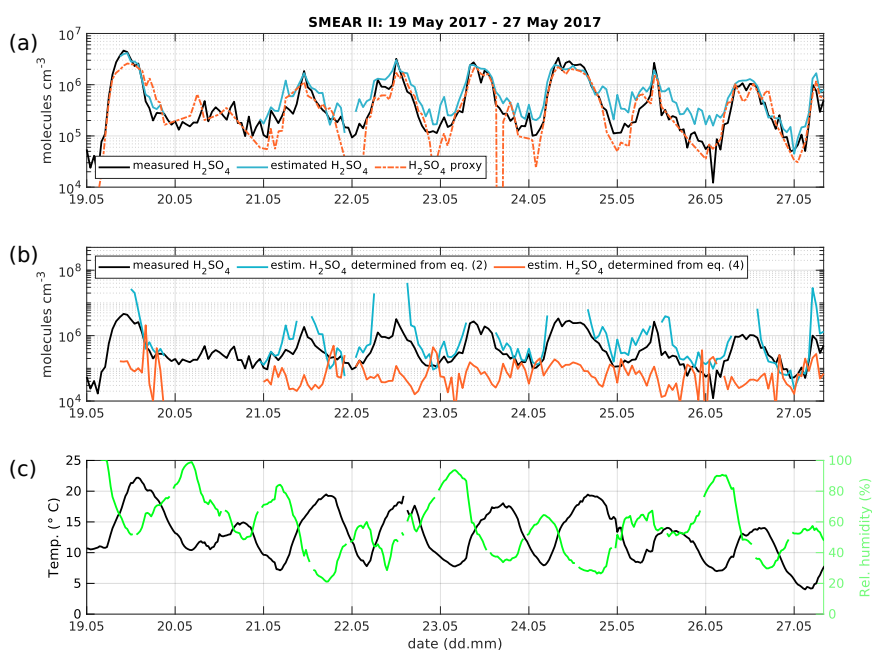
Deleted: ×

252
253
254
255
256
257

Table 1: Root mean square error (RMSE) and R^2 of the estimated H_2SO_4 concentration at the SMEAR II station and Neumayer Station III. The day- and night-time are split in 06:00 – 18:00 local time (LT) and 18:00 – 06:00 LT, respectively. For the SMEAR II station, we also show the RMSE and R^2 of the H_2SO_4 proxy calculated with the introduced method by (Dada et al., 2020).

	Root mean square error (RMSE)		
	SMEAR II		Neumayer Station III
	Estimated H_2SO_4 eq. (8)	H_2SO_4 proxy	Estimated H_2SO_4 eq. (8)
Daytime	$4.12 \times 10^5 \text{ cm}^{-3}$	$5.54 \times 10^5 \text{ cm}^{-3}$	$1.43 \times 10^6 \text{ cm}^{-3}$
Night-time	$3.23 \times 10^5 \text{ cm}^{-3}$	$4.25 \times 10^5 \text{ cm}^{-3}$	$1.63 \times 10^6 \text{ cm}^{-3}$
	R^2		
Daytime	0.85	0.78	0.48
Night-time	0.85	0.84	0.37

258

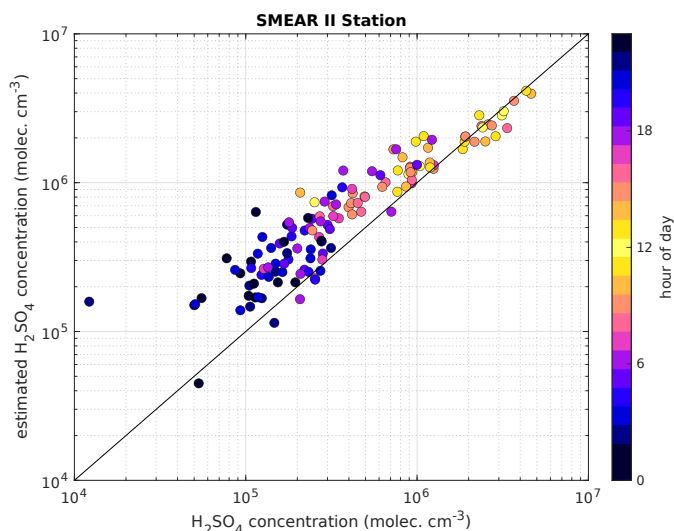


259
260
261

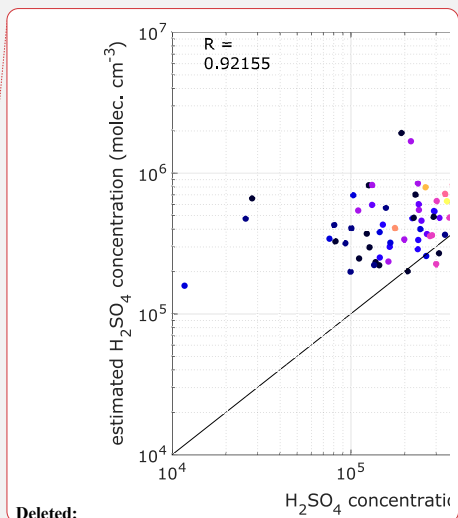
Figure 4 (a) Time series of measured H_2SO_4 concentration from the CI-APi-TOF (black) and estimated H_2SO_4 concentration from the APi-TOF (blue) and H_2SO_4 proxy from Dada et al. (2020) (orange) between 19 and 27 May 2017. The concentration

Deleted: 3
Deleted: the bisulphate ion (HSO_4^- , $SA_{monomer}$), H_2SO_4 clustered with bisulphate ($H_2SO_4 \cdot HSO_4^-$, SA_{dimer}) and two H_2SO_4 molecules clustered with the bisulphate ion ($(H_2SO_4)_2 \cdot HSO_4^-$, SA_{trimer})
Deleted: 28

268 is given in molecules cm^{-3} . (b) Measured H_2SO_4 concentration as in panel (a) in black and determined concentration from eq.
 269 2 (blue) and eq. 4 (orange). (c) Temperature and relative humidity.
 270



Deleted: ions s^{-1}
 Deleted: measured by the APi-TOF.



Deleted:

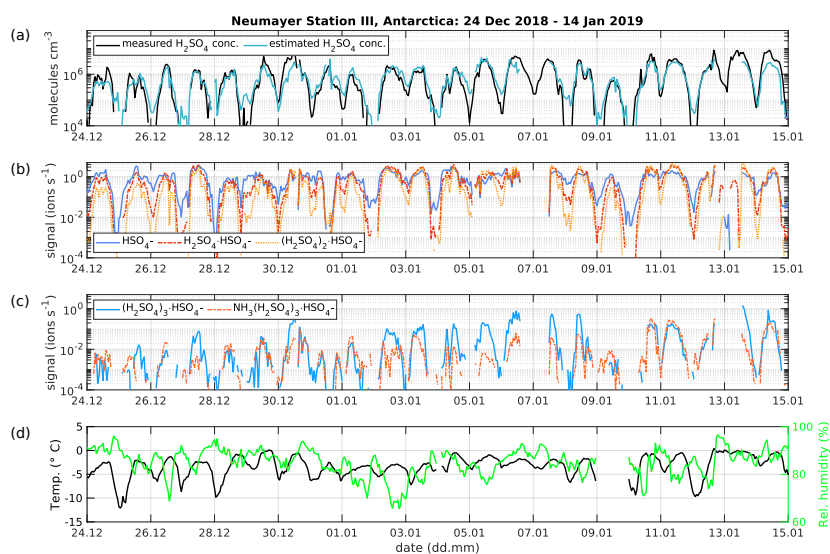
271
 272 **Figure 5** Measured H_2SO_4 concentration using a CI-APi-TOF (horizontal-axis) versus estimated H_2SO_4 concentration based
 273 on APi-TOF results (vertical-axis) at SMEAR II station. For the estimation of H_2SO_4 , the transmission efficiency was taken
 274 into account. The colour is indicating the hour of the day and the black line is the 1:1 ratio. Between 08:00 and 16:00 local
 275 time, the concentrations are agreeing well. The shown data contains the time period from 19 to 27 May 2017. The overall
 276 correlation coefficient (Pearson) is 0.94.
 277

Deleted: 4
 Deleted: x
 Deleted: y
 Deleted:).
 Deleted: 28
 Deleted: 92

278 For the sake of completeness, the estimation of the H_2SO_4 concentration determined from Eqs. 2 and 4, assuming
 279 pseudo-steady state, are depicted in Fig. 4b. The estimated H_2SO_4 concentration from Eq. 2 is highly
 280 overestimating, since the losses of the SA_{dimer} to the $\text{SA}_{\text{trimer}}$ are neglected. When solving Eq. 4 for H_2SO_4 , only
 281 the needed H_2SO_4 for the formation of the trimer is considered and the monomer and dimer production are
 282 neglected. Consequently, the resulting estimated H_2SO_4 concentration is vastly underestimating the real
 283 concentration.
 284

285 The presented method was also applied to measurements taken at the Neumayer Station III, Antarctica, in order
 286 to test it in a different environment. Here, we used the condensation sink reported by Weller et al. (2015) at
 287 Neumayer Station of $1 \times 10^{-3} \text{ s}^{-1}$. Figure 6 shows a three-week period between 24 December 2018 and 14 January
 288 2019. The calibration factor of the CI-APi-TOF used for measuring the sulfuric acid concentration is 4.9×10^9 .
 289 Here, the estimated sulfuric acid concentration underestimates the measured concentration when the $\text{SA}_{\text{tetramer}}$ and
 290 $\text{NH}_3(\text{H}_2\text{SO}_4)_3\text{HSO}_4^-$ cluster show high concentrations (Fig. 6c). A possible explanation for the underestimation
 291 might be the neglect of the growth of sulfuric acid to oligomers larger than the tetramer, as well as its clustering
 292 with bases and water (Fig. 6b and c). In coastal Antarctica, the main nucleating mechanism was observed to be

302 negative ion-induced sulfuric acid-ammonia nucleation, acting as a major sink for sulfuric acid molecules due to
 303 its clustering with bases (Jokinen et al., 2018). Including the SA_{tetramer} and SA_{tetramer} clustered with NH₃ in the
 304 estimation equation improved the correlation (R²) from 0.48 to 0.54. Nevertheless, the diurnal variation of the SA
 305 concentration is represented well by this method. During times with lower sulfuric acid concentrations, our
 306 method gives higher values than the measured concentrations (Fig. 6).



307 **Figure 6** (a) Time series of measured H₂SO₄ concentration from the CI-API-TOF (black) and estimated H₂SO₄ concentration
 308 from the API-TOF (blue) between 24 December 2018 and 14 January 2019 at Neumayer Station III, Antarctica. The
 309 concentration is given in molecules cm⁻³. (b) Time series of the bisulphate ion (HSO₄⁻, SA_{monomer}), H₂SO₄ clustered with
 310 bisulphate (H₂SO₄:HSO₄⁻, SA_{dimer}), two H₂SO₄ molecules clustered with the bisulphate ion ((H₂SO₄)₂:HSO₄⁻, SA_{trimer}) and (c)
 311 three H₂SO₄ molecules clustered with the bisulphate ion ((H₂SO₄)₃:HSO₄⁻, SA_{tetramer}) as well as the SA_{tetramer} clustered with
 312 NH₃. (d) Temperature and relative humidity measured at Neumayer Station III.

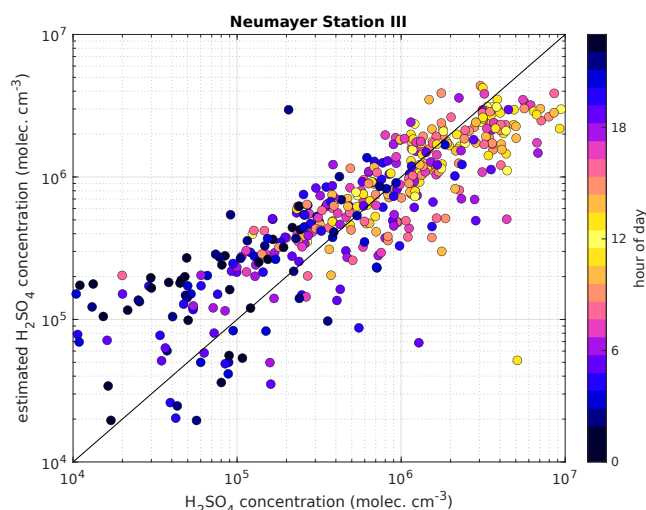


Figure 7 Measured H_2SO_4 concentration using a CI-API-TOF (horizontal axis) versus estimated H_2SO_4 concentration based on API-TOF results (vertical axis) at the Neumayer Station III. For the estimation of H_2SO_4 , the transmission efficiency was taken into account. The colour is indicating the hour of the day and the black line is the 1:1 ratio. The shown data contains the time period from 24 December 2016 to 14 January 2019. The overall correlation coefficient (Pearson) is 0.77.

4 Conclusions

Here we derived a theoretical expression to estimate H_2SO_4 concentrations based on API-TOF measurements of ambient ions. The estimation agrees well with the measured concentration during daytime in the boreal forest ($R^2 = 0.85$), indicating that the estimation is able to represent the diurnal variation and trend of H_2SO_4 concentrations during most of the time when active clustering of sulfuric acid is inducing the initial step(s) of atmospheric new particle formation. However, in an atmosphere, where sulfuric acid is the dominating pathway for initiating new particle formation, the method might underestimate the H_2SO_4 concentrations, as this method does not include the rapid clustering to bigger of sulfuric acid clusters and clustering with bases directly, e.g. in the Antarctic atmosphere ($R^2 = 0.48$; during daytime).

The API-TOF's "ion mode", i.e. direct ion sampling without chemical ionisation, remains a crucial tool in many field deployments and laboratory studies, since it is extremely sensitive and allows for observing atmospheric clustering molecule by molecule, which in most cases is impossible when relying on chemical ionization. Therefore, having available a reliable estimate of H_2SO_4 concentration allows us to utilise the API-TOF ion mode even more effectively.

Data availability

The data can be accessed via Zenodo ([10.5281/zenodo.5266313](https://doi.org/10.5281/zenodo.5266313)).

Deleted: and with high enough H_2SO_4 concentrations,

Deleted: give accurate enough

Deleted: taking as

Deleted: not yet published, the correct link and doi will follow...

346

347 **Author contribution**

348 LJB, SS, VMK and MK designed the study. LJB and MS performed the measurements. SS and LJB derived the
349 equations. LJB processed and analysed the data and performed the data visualisation. MK and VMK supervised
350 the process. All authors commented and edited the paper.

351

352 **Acknowledgements**

353 We acknowledge the following projects: ACCC Flagship funded by the Academy of Finland grant number
354 337549, Academy professorship funded by the Academy of Finland (grant no. 302958), Academy of Finland
355 projects no. 1325656, 310682, 316114, 325647 and 296628, Russian Mega Grant project “Megapolis - heat and
356 pollution island: interdisciplinary hydroclimatic, geochemical and ecological analysis” application reference
357 2020-220-08-5835, “Quantifying carbon sink, CarbonSink+ and their interaction with air quality” INAR project
358 funded by Jane and Aatos Erkkö Foundation, European Research Council (ERC) project ATM-GTP Contract No.
359 742206 and GASPARCON, grant agreement no. 714621. We thank the tofTools team for providing the tools for
360 the mass spectrometry analysis. We thank the technical and scientific staff in Hyttiälä SMEAR II and the
361 technicians and scientists of the Neumayer overwintering teams of the years 2018 and 2019. We thank Lubna
362 Dada for calculating the SA proxy for SMEAR II station. We thank Janne Lampilahti for providing the codes to
363 process the NAIS dataset.

Deleted: and

Deleted: .

Deleted: Technical

Deleted: stations is acknowledged.

368
369
370
371
372
373
374
375
376
377
378
379
380
381
382
383
384
385
386
387
388
389
390
391
392
393
394
395
396
397
398
399
400
401
402
403
404
405
406
407
408
409
410
411
412
413

References

- Arnold, F. and Fabian, R.: First measurements of gas phase sulphuric acid in the stratosphere, 283, 55–57, <https://doi.org/10.1038/283055a0>, 1980.
- Beck, L. J., Sarnela, N., Junninen, H., Hoppe, C. J. M., Garmash, O., Bianchi, F., Riva, M., Rose, C., Peräkylä, O., Wimmer, D., Kausiala, O., Jokinen, T., Ahonen, L., Mikkilä, J., Hakala, J., He, X.-C., Kontkanen, J., Wolf, K. K. E., Cappelletti, D., Mazzola, M., Traversi, R., Petroselli, C., Viola, A. P., Vitale, V., Lange, R., Massling, A., Nøjgaard, J. K., Krejci, R., Karlsson, L., Zieger, P., Jang, S., Lee, K., Vakkari, V., Lampilahti, J., Thakur, R. C., Leino, K., Kangasluoma, J., Duplissy, E.-M., Siivola, E., Marbouti, M., Tham, Y. J., Saiz-Lopez, A., Petäjä, T., Ehn, M., Worsnop, D. R., Skov, H., Kulmala, M., Kerminen, V.-M., and Sipilä, M.: Differing Mechanisms of New Particle Formation at Two Arctic Sites, *Geophysical Research Letters*, 48, <https://doi.org/10.1029/2020GL091334>, 2021.
- Birmili, W., Berresheim, H., Plass-Dülmer, C., Elste, T., Gilge, S., Wiedensohler, A., and Uhrner, U.: The Hohenpeissenberg aerosol formation experiment (HAFEX): a long-term study including size-resolved aerosol, H₂SO₄, OH, and monoterpene measurements, 3, 361–376, <https://doi.org/10.5194/acp-3-361-2003>, 2003.
- Cai, R., Yan, C., Yang, D., Yin, R., Lu, Y., Deng, C., Fu, Y., Ruan, J., Li, X., Kontkanen, J., Zhang, Q., Kangasluoma, J., Ma, Y., Hao, J., Worsnop, D. R., Bianchi, F., Paasonen, P., Kerminen, V.-M., Liu, Y., Wang, L., Zheng, J., Kulmala, M., and Jiang, J.: Sulfuric acid–amine nucleation in urban Beijing, 21, 2457–2468, <https://doi.org/10.5194/acp-21-2457-2021>, 2021.
- Dada, L., Yliviikka, I., Baalbaki, R., Li, C., Guo, Y., Yan, C., Yao, L., Sarnela, N., Jokinen, T., Daellenbach, K. R., Yin, R., Deng, C., Chu, B., Nieminen, T., Wang, Y., Lin, Z., Thakur, R. C., Kontkanen, J., Stolzenburg, D., Sipilä, M., Hussein, T., Paasonen, P., Bianchi, F., Salma, I., Weidinger, T., Pikridas, M., Sciare, J., Jiang, J., Liu, Y., Petäjä, T., Kerminen, V.-M., and Kulmala, M.: Sources and sinks driving sulfuric acid concentrations in contrasting environments: implications on proxy calculations, 20, 11747–11766, <https://doi.org/10.5194/acp-20-11747-2020>, 2020.
- Ehn, M., Junninen, H., Petäjä, T., Kurtén, T., Kerminen, V.-M., Schobesberger, S., Manninen, H. E., Ortega, I. K., Vehkamäki, H., Kulmala, M., and Worsnop, D. R.: Composition and temporal behavior of ambient ions in the boreal forest, 10, 8513–8530, <https://doi.org/10.5194/acp-10-8513-2010>, 2010.
- Eisele, F. L.: Natural and anthropogenic negative ions in the troposphere, 94, 2183–2196, <https://doi.org/10.1029/JD094iD02p02183>, 1989.
- Hari, P. and Kulmala, M.: Station for Measuring Ecosystem–Atmosphere Relations (SMEAR II), *Bor. Env. Res.*, 10, 315–322, 2005.
- Herrmann, W., Eichler, T., Bernardo, N., and Fernandez de la Mora, J.: Turbulent transition arises at Re 35 000 in a short Vi-enna type DMA with a large laminarizing inlet, Proceedings of the annual conference of the AAAR, St. Louis, MO, 6–10 October 2000.
- Hirsikko, A., Nieminen, T., Gagné, S., Lehtipalo, K., Manninen, H. E., Ehn, M., Hörrak, U., Kerminen, V.-M., Laakso, L., McMurry, P. H., Mirme, A., Mirme, S., Petäjä, T., Tamm, H., Vakkari, V., Vana, M., and Kulmala, M.: Atmospheric ions and nucleation: a review of observations, 11, 767–798, <https://doi.org/10.5194/acp-11-767-2011>, 2011.
- Jokinen, T., Sipilä, M., Junninen, H., Ehn, M., Lönn, G., Hakala, J., Petäjä, T., Mauldin III, R. L., Kulmala, M., and Worsnop, D. R.: Atmospheric sulphuric acid and neutral cluster measurements using CI-APi-TOF, 12, 4117–4125, <https://doi.org/10.5194/acp-12-4117-2012>, 2012.
- Jokinen, T., Sipilä, M., Kontkanen, J., Vakkari, V., Tisler, P., Duplissy, E.-M., Junninen, H., Kangasluoma, J., Manninen, H. E., Petäjä, T., Kulmala, M., Worsnop, D. R., Kirkby, J., Virkkula, A., and Kerminen, V.-M.: Ion-induced sulfuric acid–ammonia nucleation drives particle formation in coastal Antarctica, *Sci Adv*, 4, eaat9744, <https://doi.org/10.1126/sciadv.aat9744>, 2018.

Deleted: Page Break

Deleted: Beck, L. J., Sarnela, N., Junninen, H., Hoppe, C. J. M., Garmash, O., Bianchi, F., Riva, M., Rose, C., Peräkylä, O., Wimmer, D., Kausiala, O., Jokinen, T., Ahonen, L., Mikkilä, J., Hakala, J., He, X.-C., Kontkanen, J., Wolf, K. K. E., Cappelletti, D., Mazzola, M., Traversi, R., Petroselli, C., Viola, A. P., Vitale, V., Lange, R., Massling, A., Nøjgaard, J. K., Krejci, R., Karlsson, L., Zieger, P., Jang, S., Lee, K., Vakkari, V., Lampilahti, J., Thakur, R. C., Leino, K., Kangasluoma, J., Duplissy, E.-M., Siivola, E., Marbouti, M., Tham, Y. J., Saiz-Lopez, A., Petäjä, T., Ehn, M., Worsnop, D. R., Skov, H., Kulmala, M., Kerminen, V.-M., and Sipilä, M.: Differing Mechanisms of New Particle Formation at Two Arctic Sites, *Geophysical Research Letters*, 48, e2020GL091334, <https://doi.org/10.1029/2020GL091334>, 2021.

Birmili, W., Berresheim, H., Plass-Dülmer, C., Elste, T., Gilge, S., Wiedensohler, A., and Uhrner, U.: The Hohenpeissenberg aerosol formation experiment (HAFEX): a long-term study including size-resolved aerosol, H₂SO₄, OH, and monoterpene measurements, 3, 361–376, <https://doi.org/10.5194/acp-3-361-2003>, 2003.

Cai, R., Yan, C., Yang, D., Yin, R., Lu, Y., Deng, C., Fu, Y., Ruan, J., Li, X., Kontkanen, J., Zhang, Q., Kangasluoma, J., Ma, Y., Hao, J., Worsnop, D. R., Bianchi, F., Paasonen, P., Kerminen, V.-M., Liu, Y., Wang, L., Zheng, J., Kulmala, M., and Jiang, J.: Sulfuric acid–amine nucleation in urban Beijing, 21, 2457–2468, <https://doi.org/10.5194/acp-21-2457-2021>, 2021.

Dada, L., Yliviikka, I., Baalbaki, R., Li, C., Guo, Y., Yan, C., Yao, L., Sarnela, N., Jokinen, T., Daellenbach, K. R., Yin, R., Deng, C., Chu, B., Nieminen, T., Wang, Y., Lin, Z., Thakur, R. C., Kontkanen, J., Stolzenburg, D., Sipilä, M., Hussein, T., Paasonen, P., Bianchi, F., Salma, I., Weidinger, T., Pikridas, M., Sciare, J., Jiang, J., Liu, Y., Petäjä, T., Kerminen, V.-M., and Kulmala, M.: Sources and sinks driving sulfuric acid concentrations in contrasting environments: implications on proxy calculations, 20, 11747–11766, <https://doi.org/10.5194/acp-20-11747-2020>, 2020.

Ehn, M., Junninen, H., Petäjä, T., Kurtén, T., Kerminen, V.-M., Schobesberger, S., Manninen, H. E., Ortega, I. K., Vehkamäki, H., Kulmala, M., and Worsnop, D. R.: Composition and temporal behavior of ambient ions in the boreal forest, 10, 8513–8530, <https://doi.org/10.5194/acp-10-8513-2010>, 2010.

Hirsikko, A., Nieminen, T., Gagné, S., Lehtipalo, K., Manninen, H. E., Ehn, M., Hörrak, U., Kerminen, V.-M., Laakso, L., McMurry, P. H., Mirme, A., Mirme, S., Petäjä, T., Tamm, H., Vakkari, V., Vana, M., and Kulmala, M.: Atmospheric ions and nucleation: a review of observations, 11, 767–798, <https://doi.org/10.5194/acp-11-767-2011>, 2011.

Jokinen, T., Sipilä, M., Kontkanen, J., Vakkari, V., Tisler, P., Duplissy, E.-M., Junninen, H., Kangasluoma, J., Manninen, H. E., Petäjä, T., Kulmala, M., Worsnop, D. R., Kirkby, J., Virkkula, A., and Kerminen, V.-M.: Ion-induced sulfuric acid–ammonia nucleation drives particle formation in coastal Antarctica, *Sci Adv*, 4, eaat9744, <https://doi.org/10.1126/sciadv.aat9744>, 2018.

Junninen, H., Ehn, M., Petäjä, T., Luosujärvi, L., Kotiaho, T., Kostianen, R., Rohner, U., Gonin, M., Fuhrer, K., Kulmala, M., and Worsnop, D. R.: A high-resolution mass spectrometer to measure atmospheric ion composition, 3, 1039–1053, <https://doi.org/10.5194/amt-3-1039-2010>, 2010.

Kerminen, V.-M., Petäjä, T., Manninen, H. E., Paasonen, P., Nieminen, T., Sipilä, M., Junninen, H., Ehn, M., Gagné ... [11]

561 [Junninen, H., Ehn, M., Petäjä, T., Luosujärvi, L., Kotiaho, T., Kostianinen, R., Rohner, U., Gonin, M., Fuhrer, K.,](#)
562 [Kulmala, M., and Worsnop, D. R.: A high-resolution mass spectrometer to measure atmospheric ion](#)
563 [composition, 3, 1039–1053, <https://doi.org/10.5194/amt-3-1039-2010>, 2010.](#)

564 [Kerminen, V.-M., Petäjä, T., Manninen, H. E., Paasonen, P., Nieminen, T., Sipilä, M., Junninen, H., Ehn, M.,](#)
565 [Gagné, S., Laakso, L., Riipinen, I., Vehkamäki, H., Kurten, T., Ortega, I. K., Dal Maso, M., Brus, D.,](#)
566 [Hyvärinen, A., Lihavainen, H., Leppä, J., Lehtinen, K. E. J., Mirme, A., Mirme, S., Hörrak, U., Berndt, T.,](#)
567 [Stratmann, F., Birmili, W., Wiedensohler, A., Metzger, A., Dommien, J., Baltensperger, U., Kiendler-Scharr, A.,](#)
568 [Mentel, T. F., Wildt, J., Winkler, P. M., Wagner, P. E., Petzold, A., Minikin, A., Plass-Dülmer, C., Pöschl, U.,](#)
569 [Laaksonen, A., and Kulmala, M.: Atmospheric nucleation: highlights of the EUCAARI project and future](#)
570 [directions, 10, 10829–10848, <https://doi.org/10.5194/acp-10-10829-2010>, 2010.](#)

571 [Kontkanen, J., Lehtinen, K. E. J., Nieminen, T., Manninen, H. E., Lehtipalo, K., Kerminen, V.-M., and Kulmala,](#)
572 [M.: Estimating the contribution of ion–ion recombination to sub-2 nm cluster concentrations from atmospheric](#)
573 [measurements, 13, 11391–11401, <https://doi.org/10.5194/acp-13-11391-2013>, 2013.](#)

574 [Kuang, C., McMurry, P. H., McCormick, A. V., and Eisele, F. L.: Dependence of nucleation rates on sulfuric](#)
575 [acid vapor concentration in diverse atmospheric locations, 113, <https://doi.org/10.1029/2007JD009253>, 2008.](#)

576 [Kulmala, M., Vehkamäki, H., Petäjä, T., Dal Maso, M., Lauri, A., Kerminen, V.-M., Birmili, W., and McMurry,](#)
577 [P. H.: Formation and growth rates of ultrafine atmospheric particles: a review of observations, *Journal of*](#)
578 [*Aerosol Science*, 35, 143–176, <https://doi.org/10.1016/j.jaerosci.2003.10.003>, 2004.](#)

579 [Kulmala, M., Petäjä, T., Nieminen, T., Sipilä, M., Manninen, H. E., Lehtipalo, K., Dal Maso, M., Aalto, P. P.,](#)
580 [Junninen, H., Paasonen, P., Riipinen, I., Lehtinen, K. E. J., Laaksonen, A., and Kerminen, V.-M.: Measurement](#)
581 [of the nucleation of atmospheric aerosol particles, 7, 1651–1667, <https://doi.org/10.1038/nprot.2012.091>, 2012.](#)

582 [Kulmala, M., Petäjä, T., Ehn, M., Thornton, J., Sipilä, M., Worsnop, D. R., and Kerminen, V.-M.: Chemistry of](#)
583 [Atmospheric Nucleation: On the Recent Advances on Precursor Characterization and Atmospheric Cluster](#)
584 [Composition in Connection with Atmospheric New Particle Formation, 65, 21–37,](#)
585 [<https://doi.org/10.1146/annurev-physchem-040412-110014>, 2014.](#)

586 [Kürten, A., Rondo, L., Ehrhart, S., and Curtius, J.: Calibration of a Chemical Ionization Mass Spectrometer for](#)
587 [the Measurement of Gaseous Sulfuric Acid, *J. Phys. Chem. A*, 116, 6375–6386,](#)
588 [<https://doi.org/10.1021/jp212123n>, 2012.](#)

589 [Lehtinen, K. E. J., Dal Maso, M., Kulmala, M., and Kerminen, V.-M.: Estimating nucleation rates from apparent](#)
590 [particle formation rates and vice versa: Revised formulation of the Kerminen–Kulmala equation, *Journal of*](#)
591 [*Aerosol Science*, 38, 988–994, <https://doi.org/10.1016/j.jaerosci.2007.06.009>, 2007.](#)

592 [Lovejoy, E. R., Curtius, J., and Froyd, K. D.: Atmospheric ion-induced nucleation of sulfuric acid and water,](#)
593 [109, <https://doi.org/10.1029/2003JD004460>, 2004.](#)

594 [Lu, Y., Yan, C., Fu, Y., Chen, Y., Liu, Y., Yang, G., Wang, Y., Bianchi, F., Chu, B., Zhou, Y., Yin, R.,](#)
595 [Baalbaki, R., Garmash, O., Deng, C., Wang, W., Liu, Y., Petäjä, T., Kerminen, V.-M., Jiang, J., Kulmala, M.,](#)
596 [and Wang, L.: A proxy for atmospheric daytime gaseous sulfuric acid concentration in urban Beijing, 19, 1971–](#)
597 [1983, <https://doi.org/10.5194/acp-19-1971-2019>, 2019.](#)

598 [Mahfouz, N. G. A. and Donahue, N. M.: Technical note: The enhancement limit of coagulation scavenging of](#)
599 [small charged particles, 21, 3827–3832, <https://doi.org/10.5194/acp-21-3827-2021>, 2021.](#)

600 [Mikkonen, S., Romakkaniemi, S., Smith, J. N., Korhonen, H., Petäjä, T., Plass-Duelmer, C., Boy, M., McMurry,](#)
601 [P. H., Lehtinen, K. E. J., Joutsensaari, J., Hamed, A., Mauldin III, R. L., Birmili, W., Spindler, G., Arnold, F.,](#)
602 [Kulmala, M., and Laaksonen, A.: A statistical proxy for sulphuric acid concentration, 11, 11319–11334,](#)
603 [<https://doi.org/10.5194/acp-11-11319-2011>, 2011.](#)

604 [Mirme, S. and Mirme, A.: The mathematical principles and design of the NAIS – a spectrometer for the](#)
605 [measurement of cluster ion and nanometer aerosol size distributions, 6, 1061–1071, \[https://doi.org/10.5194/amt-\]\(https://doi.org/10.5194/amt-6-1061-2013\)](#)
606 [6-1061-2013](#), 2013.

607 [Ortega, I. K., Olenius, T., Kupiainen-Määttä, O., Loukonen, V., Kurtén, T., and Vehkamäki, H.: Electrical](#)
608 [charging changes the composition of sulfuric acid–ammonia/dimethylamine clusters, 14, 7995–8007,](#)
609 <https://doi.org/10.5194/acp-14-7995-2014>, 2014.

610 [Petäjä, T., Mauldin, I. I. I., Kosciuch, E., McGrath, J., Nieminen, T., Paasonen, P., Boy, M., Adamov, A.,](#)
611 [Kotiaho, T., and Kulmala, M.: Sulfuric acid and OH concentrations in a boreal forest site, 9, 7435–7448,](#)
612 <https://doi.org/10.5194/acp-9-7435-2009>, 2009.

613 [Schobesberger, S., Junninen, H., Bianchi, F., Lönn, G., Ehn, M., Lehtipalo, K., Dommen, J., Ehrhart, S., Ortega,](#)
614 [I. K., Franchin, A., Nieminen, T., Riccobono, F., Hutterli, M., Duplissy, J., Almeida, J., Amorim, A.,](#)
615 [Breitenlechner, M., Downard, A. J., Dunne, E. M., Flagan, R. C., Kajos, M., Keskinen, H., Kirkby, J., Kupc, A.,](#)
616 [Kürten, A., Kurtén, T., Laaksonen, A., Mathot, S., Onnela, A., Praplan, A. P., Rondo, L., Santos, F. D.,](#)
617 [Schallhart, S., Schnitzhofer, R., Sipilä, M., Tomé, A., Tsagkogeorgas, G., Vehkamäki, H., Wimmer, D.,](#)
618 [Baltensperger, U., Carslaw, K. S., Curtius, J., Hansel, A., Petäjä, T., Kulmala, M., Donahue, N. M., and](#)
619 [Worsnop, D. R.: Molecular understanding of atmospheric particle formation from sulfuric acid and large](#)
620 [oxidized organic molecules, PNAS, 110, 17223–17228, https://doi.org/10.1073/pnas.1306973110](#), 2013.

621 [Tuovinen, S., Kontkanen, J., Cai, R., and Kulmala, M.: Condensation sink of atmospheric vapors: the effect of](#)
622 [vapor properties and the resulting uncertainties, Environ. Sci.: Atmos., 1, 543–557,](#)
623 <https://doi.org/10.1039/D1EA00032B>, 2021.

624 [Wang, Z. B., Hu, M., Yue, D. L., Zheng, J., Zhang, R. Y., Wiedensohler, A., Wu, Z. J., Nieminen, T., and Boy,](#)
625 [M.: Evaluation on the role of sulfuric acid in the mechanisms of new particle formation for Beijing case, 11,](#)
626 <https://doi.org/10.5194/acp-11-12663-2011>, 2011.

627 [Weber, R. J., McMurry, P. H., Eisele, F. L., and Tanner, D. J.: Measurement of Expected Nucleation Precursor](#)
628 [Species and 3–500-nm Diameter Particles at Mauna Loa Observatory, Hawaii, 52, 2242–2257,](#)
629 [https://doi.org/10.1175/1520-0469\(1995\)052](https://doi.org/10.1175/1520-0469(1995)052), 1995.

630 [Weber, R. J., Marti, J. J., McMurry, P. H., Eisele, F. L., Tanner, D. J., and Jefferson, A.: Measured Atmospheric](#)
631 [New Particle Formation Rates: Implications for Nucleation Mechanisms, 151, 53–64,](#)
632 <https://doi.org/10.1080/00986449608936541>, 1996.

633 [Weller, R., Schmidt, K., Teinilä, K., and Hillamo, R.: Natural new particle formation at the coastal Antarctic site](#)
634 [Neumayer, 15, 11399–11410, https://doi.org/10.5194/acp-15-11399-2015](#), 2015.

635 [Yao, L., Garmash, O., Bianchi, F., Zheng, J., Yan, C., Kontkanen, J., Junninen, H., Mazon, S. B., Ehn, M.,](#)
636 [Paasonen, P., Sipilä, M., Wang, M., Wang, X., Xiao, S., Chen, H., Lu, Y., Zhang, B., Wang, D., Fu, Q., Geng,](#)
637 [F., Li, L., Wang, H., Qiao, L., Yang, X., Chen, J., Kerminen, V.-M., Petäjä, T., Worsnop, D. R., Kulmala, M.,](#)
638 [and Wang, L.: Atmospheric new particle formation from sulfuric acid and amines in a Chinese megacity, 361,](#)
639 <https://doi.org/10.1126/science.aao4839>, 2018.

640

